A Fuzzy-Logic Based Control Methodology for Secure Operation of a Microgrid in Interconnected and Isolated Modes

Hossein Ameli[1*†], Ehsan Abbasi[2], Mohammad Taghi Ameli[3] and Goran Strbac[1]

[1] *Electrical and Electronic Engineering Department, Imperial College, London, UK*
[2] *Amec Foster Wheeler, Vancouver, Canada*
[3] *Electrical and Electronic Engineering Department, Shahid Beheshti University, Tehran, Iran*

SUMMARY

Due to the global concerns regarding the climate change, integration of Renewable Energy Sources (RES) is considered as a mitigation approach in electric power generation. This requires advanced frequency and voltage control methodologies to overcome the challenges especially in microgrids. This paper presents a two-step frequency and voltage control methodology for microgrids with high penetration of variable RES. An optimized Proportional Integral controller is designed for a Superconductor Magnetic Energy Storage System (SMES) to minimize the transient frequency deviations. In cases that the SMES cannot stabilize the microgrid frequency in the isolated mode, the microgrid controller activates the next level of the frequency control. In the second level, an intelligent Fuzzy-Logic frequency controller is designed to adjust controllable loads, controllable generation units as well as carry out load shedding. In the interconnected mode, the MC is able to activate the second level in order to contribute to the system frequency control. Finally, an intelligent Fuzzy-Logic voltage controller, realized through distribution static synchronous compensator, is devised to control the voltage magnitude of the main feeders of the microgrid. In this work, a real-time operation algorithm for frequency as well as voltage control is proposed and has been tested by set of simulations on a low voltage benchmark network.

Received ...

KEY WORDS: Energy storage systems; microgrid; frequency control; voltage control; fuzzy-Logic; particle swarm optimization.

1. INTRODUCTION

After the Climate Change Conference in Paris in 2015, in many countries installing Renewable Energy Sources (RES) in order to reduce their greenhouse gases emissions is projected [1]. The integration of RES makes the operation of the power systems especially microgrids more challenging. Coordinating the optimal active and reactive power of the Distributed Generation (DG) units, Energy Storage Systems (ESSs), and loads in order to meet technical and economic objectives are the main tasks in operation of microgrids [2]. Microgrids are able to improve the economic, security of supply, and sustainability in distribution networks [3]. RES integration into microgrids requires operation methodologies in order to deal with variability of those renewable resources, such as the adaptive droop control method for the controllable resources of a DC microgrid as presented in [4]. ESSs support maintaining the balance of supply and demand in microgrid. In addition, local resources of Demand Response (DR) such as Thermostatically Controllable Loads

*Correspondence to: Electrical and Electronic Engineering Department, Imperial College, SW7 2AZ London, UK
†h.ameli14@imperial.ac.uk

(TCLs) and Electric Vehicles (EVs) are also controllable resources to be employed for frequency and voltage control of microgrids.

Many recent researches investigated the frequency and voltage control problems of microgrids especially in isolated mode from different aspects [5, 6, 7, 8, 9, 10, 11]. In [5], the capability of wind generation to participate in frequency control of an isolated microgrid is investigated. To support the voltage and frequency in microgrids, a method to control three-phase inverters with the possibility of connection to the main grid is proposed in [8]. Authors in [10], presented a primary frequency control approach through EVs in presence of RES. The suggested control system emulates the impact of generators inertia combined with a droop control. The results indicate the efficacy of this approach in order to damp the frequency deviations. In [12], a generalized droop control is designed based on the conventional voltage/frequency droops in order to regulate simultaneously the voltage and frequency in islanded microgrids. In [13], a hierarchical control strategy is proposed. As the primary control, current and voltage controllers are used. In order to mitigate DC voltage deviations a droop control is applied in the secondary control. Finally, a Proportional Integral (PI) controller for the power exchange of the microgrid and other grids is employed for the tertiary control. In [14] an enhanced control approach for Battery Energy Storage System (BESS) is designed in order to support the frequency of microgrids especially in islanded mode. A conventional droop control as the frequency controller is used for transferring the BESS active power to the microgrid. In addition, it was shown that the BESS could also provide voltage support in the microgrid. The role of ESS on Great Britain 2030 network in order to address the balancing challenges caused by integration of RES is studied in [15] and [16]. Abbasi *et al.* [17] presented an optimized scheduling method to show the effectiveness of BESS application in enhancing the operation of an isolated network where intermittent RES exist. The ESS application may be effective for a short term operation period due to limited volume of energy stored. Researchers in [18] proposed that for fast and long frequency deviations the Load Shedding (LS) procedure is very significant to sustain these deviations. From the voltage control perspective, authors in [19] proposed a voltage control algorithm of a microgrid that minimizes power losses in the grid. The results indicate the reliable performance of the proposed algorithm without information of the operation conditions and grid structure. In addition, a centralized online optimal reactive power control algorithm for microgrids is proposed in [20].

The aforementioned researches presented the effectiveness of ESSs in supporting frequency and voltage control in integration of RES. It is shown, how different control methods for ESSs could stabilize the network. But, in these studies, the inefficiency of ESSs in unbalanced supply-demand situations due to their technical characteristic limitations (i.e., efficiency, depth of discharge, power and energy capacities) is not investigated. The unbalanced supply-demand situation happens mostly in outage of different components, which are mainly generation units and transmission lines. In these cases, the ESSs are not able to properly contribute in stabilizing the network. Although, this situation has been studied in [21], however in this research a simple unrealistic network has been chosen, which makes the control of the network less challenging. In addition, the voltage stability is not considered and therefore it could not be concluded that the network is stabilized. To the best of our knowledge an intelligent regulation approach for Distribution Static Synchronous Compensator (DSTATCOM) in order to control the voltage of the different buses of the network is not presented in the literature. In this paper, frequency and voltage control of the microgrid is implemented through a Microgrid Controller (MC). In isolated operation mode of the microgrid, key MC tasks are: preserve the frequency of the microgrid in the permissible range; maintain the voltage of the main buses of the microgrid within the acceptable range. In interconnected operation mode, MC tasks are: 1) contribute to the system frequency control; 2) participate in coordinated voltage control of the grid. Provision of these services enhances the ability of the microgrid to integrate wind and solar power generation in both interconnected and isolated operation modes. A two-step frequency control methodology as well as a voltage control technique is proposed. In the first level of the frequency control, PI-controller parameters of the Superconductor Magnetic Energy Storage System (SMES) are tuned so that the frequency deviations is minimized through Particle Swarm Optimization (PSO). This procedure is not a real time adaptive tuning, as in system operation

it is not practical to change the PI parameters frequently. Therefore, the parameters are optimized for interconnected and isolated modes and is remained fixed in different scenarios. In the second level, in case that the battery cannot stabilize the network due to capacity limitation (in isolated mode), an intelligent demand management (i.e., DR and LS) procedure through Fuzzy-systems has been carried out. In the voltage control method, A Fuzzy-logic approach has been derived in order to keep the voltage magnitude of the main buses in an acceptable range. The European Low Voltage (LV) CIGRÉ benchmark network [22] is employed as a representative example of the microgrid network model in order to demonstrate the operation methodology developed in this work. Performance of the operation methodology is demonstrated by set of simulations.

2. FREQUENCY AND VOLTAGE CONTROL METHODOLOGIES FOR THE MICROGRID

In this section, the two-step frequency control and the voltage control of the microgrid are described. The algorithm of the frequency and voltage control is presented in Figure 1. In order to minimize the system frequency deviations under different microgrid configurations, parameters of the PI controller of the SMES is optimized based on minimizing the frequency deviation monitoring in the real-time operation. SMES is able to protect the distribution system and improve the dynamics of the system [23]. The PSO introduced as an optimization technique with fast convergence [24] is used for determining the PI controller parameters. In case that the frequency deviates from the nominal value after the first level control is performed, the second level of the frequency control is activated by MC. If a contingency case occurs, such as outage of a generation unit, SMES might fail to stabilize the frequency of the microgrid in the isolated mode due to storage capacity limitation. This will activate execution of the intelligent Fuzzy-Logic frequency controller that carries out stepwise control aimed and recovering the steady state frequency of the system to the nominal value.

In order to regulate voltage in the microgrid, an intelligent Fuzzy-Logic voltage controller is designed. As MC would detect voltage deviations, this controller would be activated. The Fuzzy-Logic voltage controller will drive the operation of DSTATCOM. This device is engaged to mitigate the voltage fluctuations. As it is reported in [25] this device is applied in order to improve the LV network voltage profile. The configuration of a DSTATCOM including the inner controllers are presented in detail in many researches such as in [26] and [27].

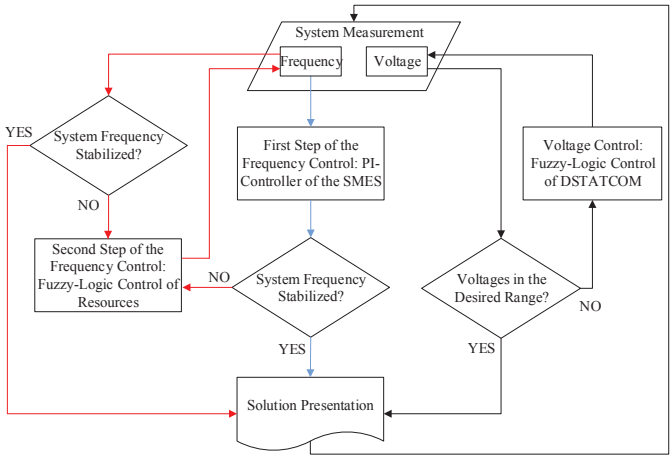

Figure 1. Real-time operation algorithm of the microgrid: first level of the frequency control by PI controller of the BESS (light blue line); second level of the frequency control by Fuzzy-Logic control of the resources of active power (red line); and voltage control by Fuzzy-Logic control of the resources of reactive power

The microgrid parameters of frequency deviation and voltage magnitude of the buses are measured. Both frequency control loop and the voltage control loop are active and monitor frequency and voltage of buses inside the microgrid. In the first level of the frequency control, the designed PI controller, which minimizes the frequency deviations by controlling the SMES

is applied. As mentioned previously, the PI controller parameters are optimized in certain circumstances and adaptive parameter tuning is not possible. In cases that the SMES fails to stabilize the microgrid frequency in isolated mode or the deviation of the system frequency in interconnected mode is significant, the intelligent Fuzzy-Logic frequency controller is activated by MC. This second level of the frequency control is applied through generation power level change , sources of DR, and LS. The concept of demand side management including DR and LS was developed in [18]. The advantage of the proposed method is that in a very short time the amount of the DR or LS is determined. The MC could act accurately and quickly through this intelligent solution to save the network. The first level of the frequency control by the SMES is by analogy similar to the primary control reserve in power systems whereas the second level of the frequency control acts similar to the secondary control reserve or the Load Frequency Control (LFC) in power systems. This analogy from the large power system is applied in the frequency control of the microgrid. The frequency control in the isolated mode is a security service to serve the microgrid. However, in the interconnected mode, the microgrid has the possibility of a coordinated operation through a Virtual Power Plant (VPP) to provide the frequency regulation service. The VPP provides visibility of the services provided by the microgrid to the electricity market and system operator. This coordinated operation requires communication between the control center of the VPP and the MC.

In the real-time operation of the microgrid, the voltage magnitude of the main feeders of the microgrid should be in a permissible range. In cases that this voltage constraint is violated, the intelligent Fuzzy-Logic voltage controller acts. The two-step frequency control and the voltage control are described in detail in the following.

In interconnected mode operation, each DG system is usually operated to provide or inject a set power to the grid, which is the current control mode in stiff synchronization with the grid [28]. When the microgrid is cut off from the main grid, each DG system has to detect this islanding situation and one of the inverters has to be switched to a voltage control mode to provide constant voltage to the local loads [29].

2.1. First level of the Frequency Control: PI Control of Energy Storage Systems

The parameters of the PI controller of the SMES is optimized through PSO based on frequency deviation monitoring in the real-time operation. The objective of this optimization is to minimize the system frequency deviations under different microgrid operation modes. In real operation system retuning the PI controller parameters frequently is implausible. Therefore, the parameter optimization is done when the operation mode of the microgrid (i.e., interconnected and isolated) has been changed. The basic reason that PSO is chosen in comparison to other intelligent methods is the implementation simplicities. Some of the other advantages of PSO are as follow [24]: More robust and flexible control can be achieved because of using probability rules, high accuracy, not using of complex operations, and considerable less optimization time in comparison to the others such as Genetic Algorithm (GA). In [30] the performance of PSO-based control is carried out.

PSO method is a multi-agent search technique [21]. In a PSO system, particles fly inside a multi-dimensional search space. During flight, each particle fits its position by virtue of its own experience and the experience of neighboring particles, making use of the best position met by itself and its neighbors. The modified velocity (1) and position (2) of each particle, the constriction factor k_a (3), and inertia weight factor β (4), are presented as follows:

$$s_{(d+1)} = k_a \times (a_1.rnd(l) \times (C_{\text{best}} - c_d) + a_2.rnd(l) \times (G_{\text{best}} - c_d) + \beta \times v_d) \tag{1}$$

$$c_{(d+1)} = c_d + s_{(d+1)} \tag{2}$$

$$k_a = \frac{2}{\left|2 - a - \sqrt{(a_2 - 4a)}\right|} \tag{3}$$

$$\beta = \beta_{\max} - (\frac{\beta_{\max} - \beta_{\min}}{\rho_{\max}}) \times \rho \tag{4}$$

In these equations, s and c are defined as its proper flight speed (velocity) and particle coordinates (position) in a search space, respectively. $C_{\rm best}$ is the best previous position of a particle. In addition, $G_{\rm best}$ is the symbol of the index of the best particle between all the particles in the group. To ensure the convergence of PSO, the use of a constriction functions are significant. d is the iteration number, s_d is the speed of particle at d-th iteration, c_d is the current position of particle, a_1 and a_2 are acceleration constants, $rnd(l)$ is a random value in range of [0,1]. a is the sum of acceleration constants and it should be larger than four. Suitable selection of β, leads to finding faster the global optimum. $\rho_{\max}$ is the maximum number of iterations, and ρ is the current number of iterations. More description regrading the PSO formulation is presented in detail in [31].

The objective of the designed PSO PI controller is to minimize the frequency deviation of the network by optimal tuning of PI controller of the of SMES in presence of RES. The optimization is done through minimizing of the integral of the the absolute value of frequency deviations (5):

$$Z = \int_{\mathbf{T}} |\Delta f_t| \cdot dt \tag{5}$$

where $\mathbf{T}$ is the time horizon, Z is the objective function, and Δf_t is the system frequency deviations.

Constraints of the microgrid include the power flow balance (6), upper and lower limits of generation units (7), power and energy capacity limitations of the storage technologies (8)-(9) were considered.

$$\forall t \in \mathbf{T}: \quad \sum_{g=1}^{N_g} P_{\rm g,t} + \sum_{s=1}^{N_s} P_{\rm s,t} = \sum_{d=1}^{N_d} P_{\rm d,t} \tag{6}$$

where $P_{g,t}$ is the generation power, $P_{s,t}$ is the power provided through storages and $P_{d,t}$ is the demand power. N_g, N_s, and N_d indicate the number of generation units, storage technologies and demands, respectively.

$$\forall g \in N_g, t \in \mathbf{T}: \quad \underline{P_{\rm g}} \leq P_{\rm g,t} \leq \overline{P_{\rm g}} \tag{7}$$

$$\forall s \in N_s, t \in \mathbf{T}: \quad P_{\rm s-} \leq P_{\rm s,t} \leq P_{\rm s+} \tag{8}$$

$$\forall s \in N_s, t \in \mathbf{T}: \quad E_{\rm s,t} \leq \overline{E_{\rm s}} \tag{9}$$

where $\underline{P_{\rm g}}$ and $\overline{P_{\rm g}}$ are the power generation capacity, $P_{\rm s-}$ and $P_{\rm s+}$ are the operational limits of storages. $\overline{E_{\rm s}}$ is the energy capacity of the storage. $E_{\rm s,t}$ is defined as energy level of storage. In operation of the microgrids, many issues such as communication delay between the components and MC [32], time delay of the ESSs, and time delay of the power electronic interfaces will influence the power balance. Thus, equation (6) changes to (10), which ΔP_t is the amount of power unbalance in the microgrid. This leads to the frequency deviations in the network.

$$\forall t \in \mathbf{T}: \quad \sum_{g=1}^{N_g} P_{\rm g,t} + \sum_{s=1}^{N_s} P_{\rm s,t} - \sum_{d=1}^{N_d} P_{\rm d,t} = \Delta P_t \tag{10}$$

As mentioned previously, in some contingency cases although the PI controller parameters are optimized but due to the technical characteristic limitation (i.e., efficiency, depth of discharge, power and energy capacities) of ESSs, the controller is not able to track the power changes. This will lead to system instability. Therefore, providing a backup controller in order to save the network from collapse is necessary.

2.2. Second level of the Frequency Control: Intelligent Fuzzy-Logic Control of Flexible Loads and Controllable Generators

One of the significant characteristics of Fuzzy systems is that they are based on human minds knowledge [33]. In addition, the concept of Fuzzy-Logic is easy to understand and is highly flexible. The ability to model nonlinear functions is another feature of Fuzzy systems. Based on these advantages and the fast reaction of these systems for decision making, Fuzzy-Logic method is chosen in this research. Many researches such as [34]-[35] study the role of Fuzzy systems in control of power systems from different perspectives and the efficacy of this method is demonstrated.

As it was presented in Figure 1, in case that the first level frequency control of the microgrid fails to stabilize the frequency, the second level of the frequency control, Fuzzy-Logic frequency controller, is activated. This controller will react in order to compensate larger frequency deviations from the reference frequency. This reaction is done through changing the power level of the generation power. In cases that controllable units fail to stabilize the frequency due to slow response of resources or inadequacy of generation or excess generation, DR and LS is considered. The DR and LS mechanisms are prioritized in the microgrid by MC. Flexible loads such as EVs and TCLs are among the potential candidates for the DR.

The first input of the Fuzzy-Logic frequency controller is related to the Area Under Curve (AUC) of the frequency. The AUC is mathematically the value of integral of the frequency deviation. For instance, if the frequency drops, the amount of this index, should increase in time. The amount of AUC depends on the slope of the drop. The slope of the frequency change indicates the severity of the incident, as it shows how fast the microgrid is going to instability. Therefore, various actions of MC are required to save the network from collapse. To realize the needed action of MC, eight membership functions based on the slope are defined. In order to quantify the range of the membership function, the simulations are run for a short time and afterwards the AUC in different operation modes are calculated. Low Frequencies (LF1 to LF5), Normal Frequency (NrF), and Over Frequencies (OF1 and OF2) which they present the amount of AUC of frequency deviations. Better operation of the microgrid is related to closer amount of AUC to zero. For instance, as it can be seen in Figure 2 (a), if the integral of the frequency deviation is not between -0.08 to 0.12 and the SMES is operating in maximum, the PI controller cannot stabilize the network. The second input is the power of the SMES; Maximum Injected Power (MIP), Normal Operation (NrO), and maximum Stored Power (MSP) of SMES (Figure 2 (b)).

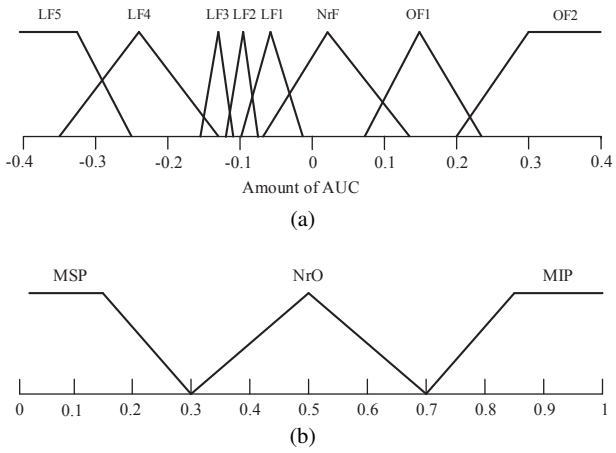

Figure 2. Membership functions of the inputs variables of the Fuzzy-Logic frequency controller: (a) SMES operational power, (b) AUC of frequency response

Different solutions based on the inputs are presented in Figure 3. The decision rules are defined in Table I. In different steps of LF, the solutions are related to DR+ and LS because of the lack of supply in comparison to consumption. The abbreviations are as follow: "DR+" for Positive Demand Response, "LLS" for Low Load Shedding, "MLS" for Medium Load Shedding, "HLS" for High

Load Shedding. In the last step, in which "LF5" and "MIP" is happened, loss of supply occurs and the whole system is shut down. The abbreviation of "DR-" means Negative reserve of Demand Response. Potential options for this purpose are TCLs. The abbreviation of "NrO" means that the situation of the system is normal and reaction of MC for the second step is not needed. Finally, "RG" means that in this situation, the supply is more than demand, hence the generation should be reduced.

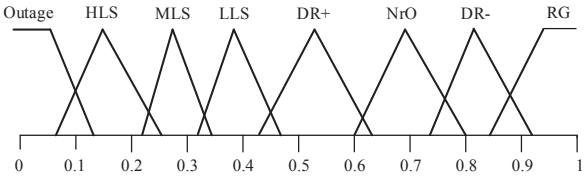

Figure 3. Membership functions of the output variable of the Fuzzy-Logic frequency controller

Table I. Rules of the Fuzzy-Logic frequency controller

AUC / ESS	MSP	NrO	MIP
LF5	NrO	NrO	Outage
LF4	NrO	NrO	HLS
LF3	NrO	NrO	MLS
LF2	NrO	NrO	LLS
LF1	NrO	NrO	DR+
NrF	NrO	NrO	NrO
OF1	DR-	NrO	NrO
OF2	RG	NrO	NrO

2.3. Voltage Control: Fuzzy-Logic Voltage Control of Resources of Reactive Power

In this controller, the voltage of different buses are considered as inputs. All of these inputs have five membership functions which is shown in Figure 4 (a). It is worth mentioning that the base voltage is 400 V. These membership functions which are Very Low Voltage (VLV), Low Voltage (LV), voltage that is in the acceptable range (NV), High Voltage (HV) and Very High Voltage (VHV), are defined for the main feeders of the microgrid. To operate the network properly, the voltage of the main feeders should be maintained between 0.95 pu and 1.05 pu.

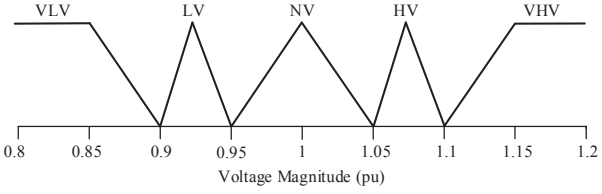

(a)

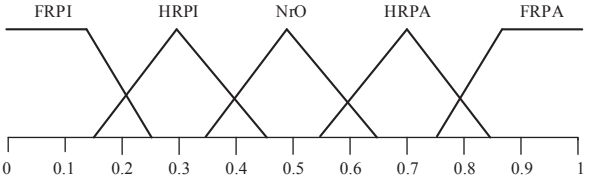

(b)

Figure 4. Membership functions of the input and output variables of the Fuzzy-Logic voltage controller: (a) Voltage magnitude in pu, (b) DSTATCOM connection

The voltage controller is realized by Fuzzy-Logic control of the DSTATCOM. The solutions are shown in Figure 4 (b). The abbreviations of the solutions are as follow: "FRPI" as Full capacity

Reactive Power Injection, "HRPI" as Half capacity Reactive Power Injection, "HRPA" as Half capacity Reactive Power Absorption, and "FRPA" as Full capacity Reactive Power Absorption. As it was mentioned, beside the DSTATCOM the BESS supports the voltage mode in isolated mode as well. The application of these controllers will be evaluated in the Numerical Results Section. The rules of the Fuzzy-Logic voltage controller is shown in Table II. It is worth mentioning that the "Mamdani" mechanism is used for the Fuzzy-logic frequency and voltage controls.

Table II. Rules of the Fuzzy-Logic voltage controller

Voltage Magnitude	Solution
VLV	FRPI
LV	HRPI
NV	NrO
HV	HRPA
VHV	FRPA

3. SET-UP OF THE MICROGRID AND DESIGN OF THE CONTROLLERS

3.1. Characteristics

The CIGRÉ European LV benchmark network [22] is selected to represent the microgrid under study. The single line diagram of the test system which is shown in Figure 5 includes sources such as PV panels, and storage systems such as BESS and SMES. There is a communication link between the resources of the microgrid and the MC. The introduced bench network [22] is designed for studying different microgrid scenarios. In this research, the focus is to study the impact of RES integration to the microgrid and therefore conventional technologies (e.g., Diesel generator) are not taken into account. The total installed capacity of the PV panels, BESS, SMES, and EVs are presented in Table III. It is worth mentioning, this network is used to study the operation of a microgrid in different configurations. The planning of the microgrid, including the placement of the components (i.e, generation technologies, ESSs, EVs, and DSTATCOM) is not considered.

Table III. Installed DG and ESS capacities in the network

Source	Capacity (kW)
BESS	200
PV panels	60
SMES	60
EV	40

3.2. Implementation of the Frequency Control of the Microgrid

The power balance in the microgrid should be maintained. Equation (11) is expressed here by the sum of the active power delivered form the main grid to the microgrid, P_t^{G}, output active power of photovoltaic generation, P_t^{PV}, active power of BESS, P_t^{BESS}, active power of SMES, P_t^{SMES}, charging power of EVs, P_t^{EVs} (value of ESS and EVs could be negative or positive):

$$\forall t \in \mathbf{T}: \quad P_t^{\mathrm{Grid}} + P_t^{\mathrm{PV}} + P_t^{\mathrm{BESS}} + P_t^{\mathrm{SMES}} + P_t^{\mathrm{EVs}} - \sum_{1}^{N_d} P_{\mathrm{d,t}} = \Delta P_t \tag{11}$$

The frequency deviation is calculated by:

$$\forall t \in \mathbf{T}: \quad \Delta f_t = \frac{\Delta P_t}{K^{\mathrm{SYS}}} \tag{12}$$

where K_{SYS} is the system frequency characteristic. In non-ideal form, a system time delay is also taken into account (13). The SMES is modeled by a first-order transfer function with the amount

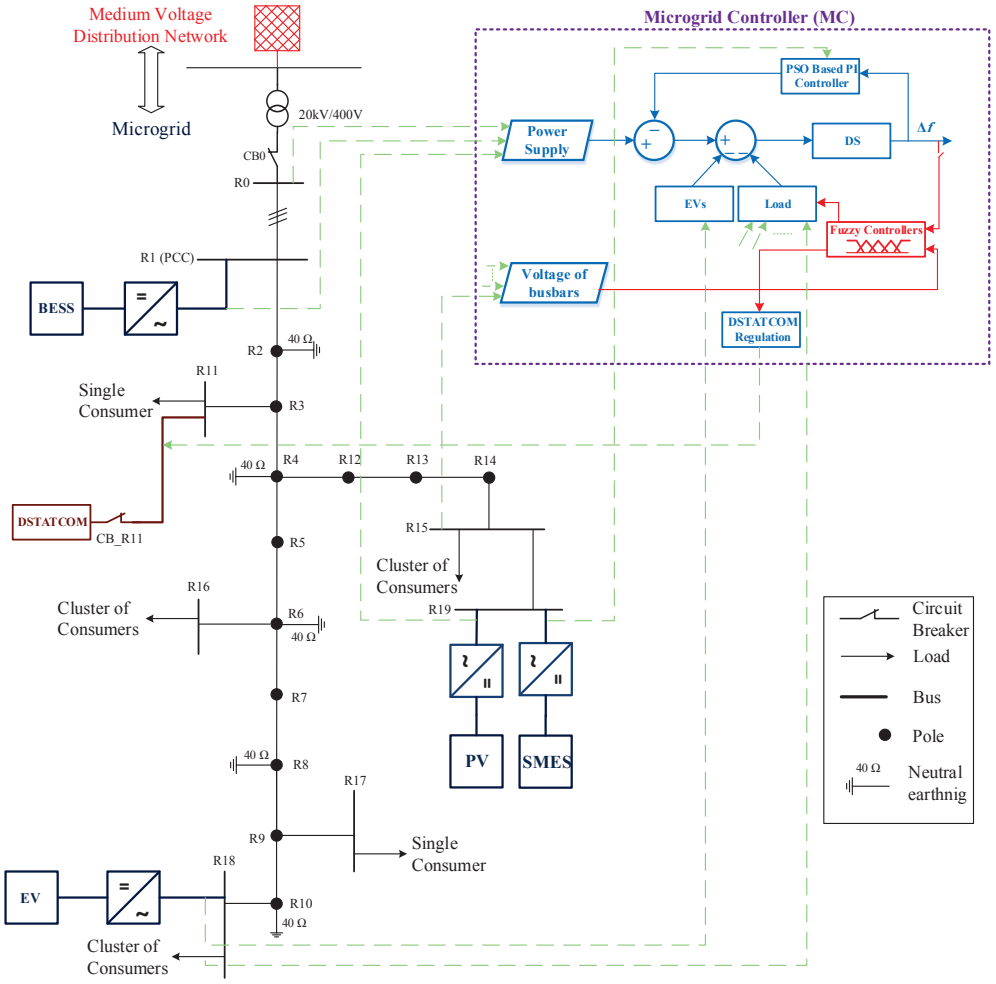

Figure 5. LV microgrid distribution benchmark network [22] with the proposed microgrid controller including frequency and voltage controllers

of 0.12 and 0.03 for the gains and time constants, respectively (13) [36]. The parameters of the microgrid are presented as M, the equal inertia constants of the generators and D as the effects of the system loads [37] which are chosen 0.2 and 0.012, respectively (14) [38].

$$\forall t \in \mathbf{T}: \quad \Delta f_t = \frac{\Delta P_t}{K^{\mathrm{SYS}}.(1+T.s)} = \frac{\Delta P_t}{D+M.s} \tag{13}$$

$$\forall t \in \mathbf{T}: \quad \Delta P_t^{\mathrm{SMES}} = \frac{K^{\mathrm{SMES}}}{(1+T^{\mathrm{SMES}}.s)}.\Delta f_t \tag{14}$$

In Figure 5 the MC including the two-step frequency control and the voltage control is presented. In the voltage control procedure, the voltage of the main buses are measured and given as input to the Fuzzy voltage controller. Then, based on the decision rules in Table II, the DSTATCOM is properly regulated in order to maintain the voltage of the buses in the permissible range. In the first level of the frequency controller Δf is given as the input to the PSO based PI controller in order to optimize the PI parameters. In contingency modes in which the PSO PI controller is not able to stabilize the network, the Fuzzy-Logic frequency controller (second level) is activated. This is

done to save the network from instability. Disturbances could have an impact on the measurements. Hence, the proposed noise cancellation module in [39] is applied to omit the disturbances.

4. NUMERICAL RESULTS

The residential network of the European LV CIGRE benchmark network in microgrid form is used for the simulations. The peak load of the network is 204 kVA [22]. In this part, in order to validate the presented frequency and voltage control methods, different scenarios are defined as follow:

Normal Operation

- The transition from the interconnected to isolated mode (Case A)
- Isolated mode of the microgrid (Case B)

Contingency Mode

- Outage of the PV panels in the isolated mode (Case C)
- Inadequacy of supply in the isolated mode (Case D)

4.1. The Transition from the Interconnected to Isolated Mode

In this case study, at time 3.3 seconds because of a fault, the microgrid is disconnected from the main grid. Therefore, the injected active and reactive power of the main grid to the microgrid descended to zero. The grid active power is shown in Figure 6.

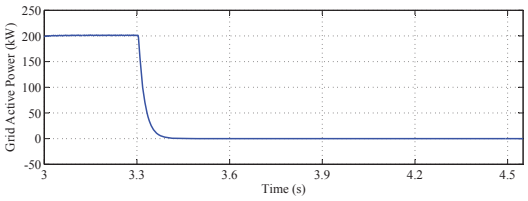

Figure 6. Injected grid power to the microgrid in kW in Case A

As it was mentioned, the control structure of the BESS should be switched from current control mode to voltage control mode to serve as a voltage source. It is noteworthy, that other storage systems and PV generation operate in current control mode to share the current, as required. When the BESS control mode is switched from current control to voltage control mode, the BESS plays the most important role in providing the required active and reactive power. This switch mode is done to keep the balance between the generation and the consumption power. The optimized proportional and integral parameters for the SMES PI controller are 21.1 and 99.8, respectively.

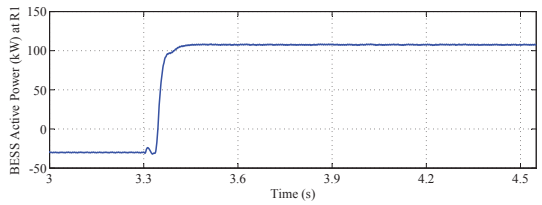

(a)

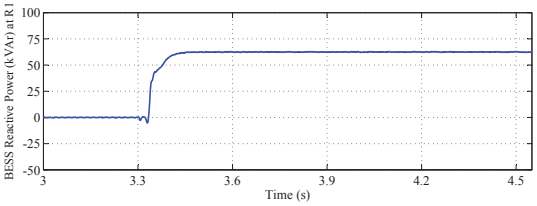

(b)

Figure 7. BESS (R1) powers in kW and KVAr in Case A

In this case, the amount of power through BESS changes from -40 kW to 105 kW. The negative sign means that the BESS stores power. As it can be seen in Figure 7 (a), it takes about 0.1 seconds that the control mode of the BESS (R1) completely changes, which is related to the time delay of the system. The time delay is related to the integration of the ESSs and PV panels through power electronic devices such as thyristors which are not ideal. Similar to active power of BESS (R1), the reactive power of BESS (R1) includes a time delay Figure 7 (b). In contrast to the interconnected mode in which EVs are charging at the aggregate power of 5 kW, in the islanded mode, those EVs should inject 30 kW power to the network and operate in Vehicle-to-Grid (V2G) mode. This change in active power which is shown in Figure 8 , includes a small oscillation due to the mode changing and also a 0.15 seconds time delay which is related to battery structure and the integration via power electronic interfaces. Detailed modeling of EVs including the charging and discharging program was out of scope of this research. Here, it is assumed that EVs are managed centralized by the MC to show how EVs could participate in the proposed control strategies.

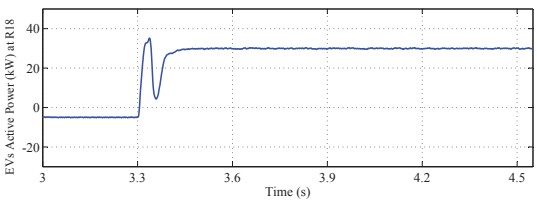

Figure 8. EVs (R18) power in kW in Case A

The SMES plays an important role in the frequency control application. This component helps the frequency control to mitigate small frequency deviations in the steady state mode. The performance of the SMES is shown in Figure 9 (a). As it can be seen in Figure 9 (b), the frequency of the system is completely recovered to 50 Hz after 0.35 seconds. This goal is achieved thanks to the timely power providing of the BESS and EVs as well as SMES participation in the frequency control application.

4.2. Isolated Mode of the Microgrid

In the isolated mode, no incident takes place, therefore, all of the components are in their steady state mode with small oscillations. The optimized proportional and integral parameters for the SMES PI controller are 23.4 and 101.7, respectively.

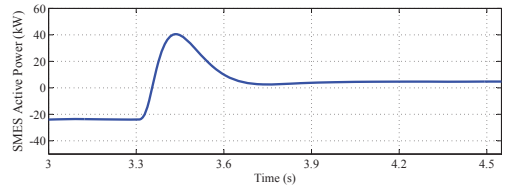

(a)

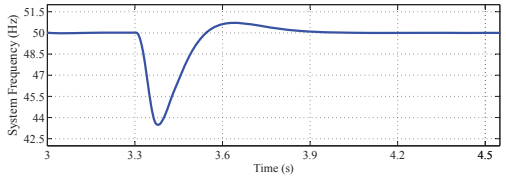

(b)

Figure 9. (a) SMES active power in kW, (b) system frequency in HZ in Case A

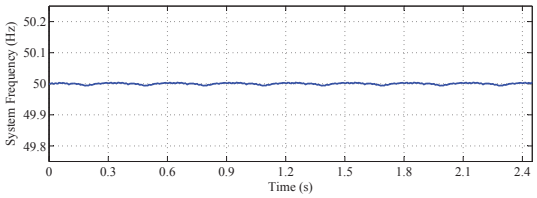

Figure 10. Frequency of the network in Case B (Islanded mode)

In this case, the maximum voltage magnitude (Bus R1) and the minimum voltage magnitude (Bus R17) are 1.00 pu and 0.95 pu, respectively. The voltage magnitudes are in the desired range, therefore, the Fuzzy-Logic voltage controller does not propose any solutions. The LFC indicates that the PV and storages provide the load consumption sufficiently and the frequency is 50 Hz. The power injection of the components in isolated mode is presented in Table IV. The frequency response is presented in Figure 10.

Table IV. Power Injection of the Components in Case B

Components	Generated/Injected Power
PV Active Power	55 (kW)
BESS Active Power	106 (kW)
BESS Reactive Power	62 (kVAr)
EVs Active Power	30 (kW)
SMES Active Power	5 (kW)

4.3. Outage of the PV Panels in the Isolated Mode

In this case study, outage of the PV panels is studied. This outage can happen either by the failure of PV panels or due to an unpredictable change in weather conditions. To study a contingency situation, this case is studied in the isolated mode. In order to present the trend of different components in detail, a short time interval around the incident is considered.

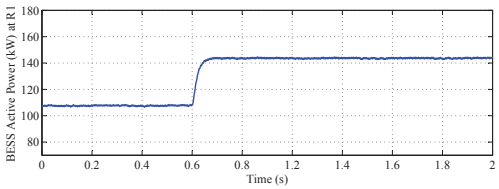

(a)

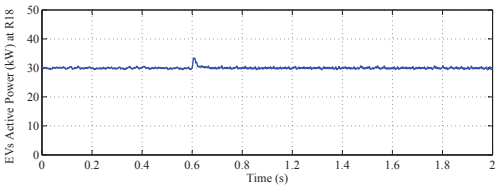

(b)

Figure 11. (a) BESS (R1) active power in kW and (b) EVs (R18) power in Case C

The time duration of the study is 2 seconds. The incident is happened at 0.6 seconds. According to Figure 5, the PV panels are connected to the bus R19 which is at the end of the feeder. As it is presented in Figure 11 (a), thanks to the role of the BESS (R1) which it is in voltage control mode, a share of PV panels active power injection, which is lost, is compensated. In 0.6 seconds, the injected power of BESS (R1) changes from approximately 105 kW to 140 kW. The EVs are operating still in V2G mode and inject 30 kW power to the microgrid (11 (b)). As it can be observed in Figure 12 (a), similar to the previous case, the SMES provides timely the extra power in order to enhance the controllability of the system through compensating the rest of the lost generation. The small oscillations of the SMES power due to the deviations of RES could be seen in the detail (Figure 12 (b)). As it is shown in Figure 12 (c), at the incident time, 0.6 seconds, a frequency drop is observed which is slightly above 1 Hz. After 0.8 seconds, the frequency is completely recovered to its nominal value. The Fuzzy-Logic frequency controller, does not propose any extra solution due to the fact that the first level of the controller stabilize the network.

Similar to the previous case studies, as input of the Fuzzy-Logic voltage controller, the voltage magnitudes of the buses are chosen. In this case study, after incident, the minimum voltage magnitude of the system is about 0.92 pu. According to Figure 4 (a), the membership function of the controller is LV. For this membership function, the proposed solution of the controller (see Table II) for the DSTATCOM is HRPI at time 0.9 seconds. The DSTATCOM is installed at bus R11 (see Figure 5) locating in the middle of the feeder for steady state voltage drop. To have an exact comparison between the voltages, Figure 13 is presented. For the dashed line it is assumed the Fuzzy system is not applied to the system. Sue to the Fuzzy-logic voltage controller application the voltage magnitude is recovered back to the acceptable range of 0.95-1.05 pu. This comparison indicates that Fuzzy-Logic voltage controller works properly and the proposed solution was sufficient to control the voltage of the buses.

4.4. Inadequacy of Supply in Isolated Mode

In this subsection, the role of DR or LS in the second level of the frequency control by Fuzzy-Logic controller is studied. This case study is similar to the Case C. The only difference here is that the capacity of SEMS in this set-up is more limited rather than in Case C, i.e., 16 kW. As it was predictable, in 0.6 seconds the frequency of the system is dropped due to the failure of the PV panels. This tends to a loss of synchronism. In this situation, the Fuzzy-Logic frequency controller is activated to overcome the situation. According to the method description in this paper, after 0.24

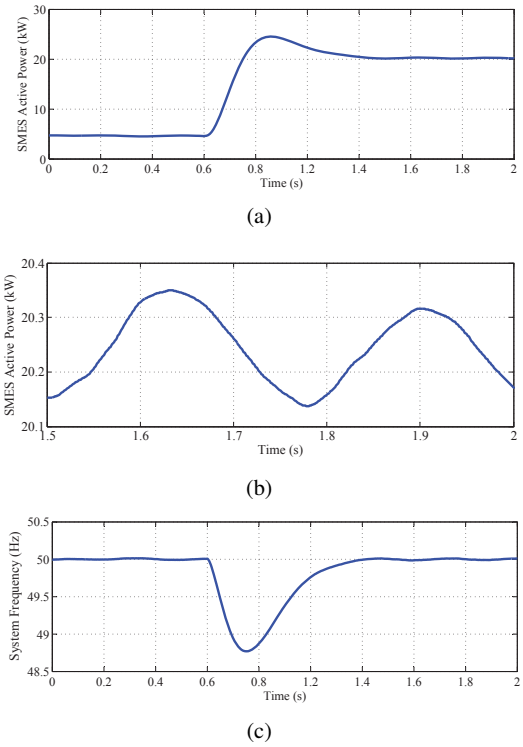

Figure 12. (a) SMES active powers in kW, (b) SMES active power in kW (in detail), (c) system frequency in Hz in Case C

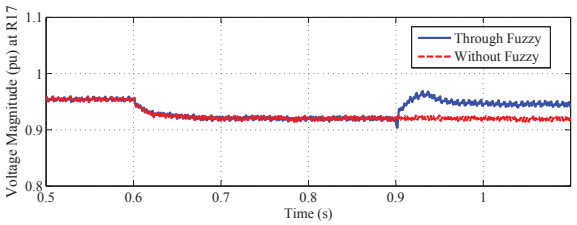

Figure 13. Comparison of the voltage magnitudes of bus R17 in pu in Case C (base voltage: 400 V)

seconds of the incident, the membership function is DR+, which means 0-7 % load management which is related to the controllable loads such as TCLs.

The comparison of the SMES active power and frequency of the system before and after DR is shown in Figure 14. As it is shown in Figure 14 (a) the SMES operates in its maximum capacity for about 1.3 seconds. After the activation of the Fuzzy-Logic frequency controller, the SMES power set-point is reduced in order to have enough free capacity available for mitigation of small frequency deviations in the steady-state mode. The stabilization is achieved after about 1.4 seconds. The frequency response indicates the sufficient reaction of MC at 0.24 seconds by the Fuzzy-Logic frequency controller. As it was concluded from Case D, the SMES with the PSO PI controller is not able to control the frequency due to the capacity limitation of SMES. Thus, as a backup the Fuzzy-Logic frequency controller is proposed. Through the case studies, the efficacy of the Fuzzy-Logic voltage and frequency controllers in saving the network from collapse is quantified and validated.

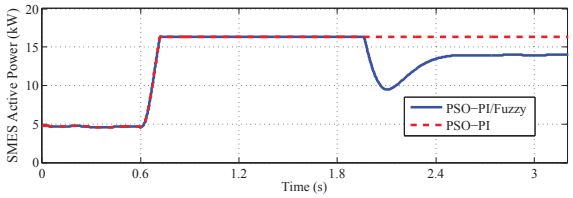

(a)

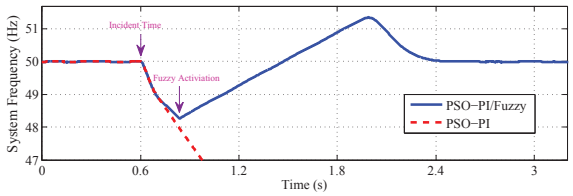

(b)

Figure 14. (a) SMES active power in kW, (b) system frequency in Hz in Case D

5. CONCLUSION

This paper proposed a real-time operation methodology for the frequency and voltage control of a microgrid in interconnected and isolated modes. An interconnected and isolated operation objectives has been defined for the microgrid. A two-step frequency control has been proposed to cover a full frequency control required in real-time operation of a microgrid. In the first level of the frequency control, the SMES through a PI controller with optimized parameters of the controller mitigates small frequency fluctuations. The parameters are calculated, so that the frequency deviations is minimized using the PSO method. In the second level of the frequency control, a Fuzzy-Logic based frequency control is activated in case that the first level fails to stabilize the frequency due to ESS capacity restriction. A Fuzzy-Logic voltage controller has been devised for DSTATCOM in order to support the voltage of the main feeders of the microgrid. The CIGRÉ European Low Voltage Benchmark Network is chosen to represent the proposed microgrid. The control methodologies in different operation modes of the microgrid has been tested and their effectiveness has been demonstrated.

ACKNOWLEDGMENTS

The authors would like to thank the institute of Sustainable Electric Networks and Sources of Energy (SENSE) at Technische Univerisaet Berlin for providing the required software and research facilities.

REFERENCES

1. E. Xydas, M. Qadrdan, C. Marmaras, L. Cipcigan, N. Jenkins, H. Ameli, Probabilistic wind power forecasting and its application in the scheduling of gas-fired generators, Applied Energy 192 (2017) 382 –394.
2. D. Papadaskalopoulos, D. Pudjianto, G. Strbac, Decentralized coordination of microgrids with flexible demand and energy storage, Sustainable Energy, IEEE Transactions on 5 (4) (2014) 1406–1414.
3. I. G. Sardou, M. E. Khodayar, K. Khaledian, M. Soleimani-damaneh, M. T. Ameli, Energy and reserve market clearing with microgrid aggregators, IEEE Transactions on Smart Grid 7 (6) (2016) 2703–2712.
4. K. Strunz, E. Abbasi, D. N. Huu, Dc microgrid for wind and solar power integration, Emerging and Selected Topics in Power Electronics, IEEE Journal of 2 (1) (2014) 115–126.
5. I. Margaris, S. Papathanassiou, N. Hatziargyriou, A. Hansen, P. Sorensen, Frequency control in autonomous power systems with high wind power penetration, Sustainable Energy, IEEE Transactions on 3 (2) (2012) 189–199.

6. M. Taghizadeh, M. Hoseintabar, J. Faiz, Frequency control of isolated wt/pv/sofc/uc network with new control strategy for improving sofc dynamic response, International Transactions on Electrical Energy Systems 25 (9) (2015) 1748–1770.
7. A. Bidram, A. Davoudi, Hierarchical structure of microgrids control system, Smart Grid, IEEE Transactions on 3 (4) (2012) 1963–1976.
8. J. Vasquez, J. Guerrero, M. Savaghebi, J. Eloy-Garcia, R. Teodorescu, Modeling, analysis, and design of stationary-reference-frame droop-controlled parallel three-phase voltage source inverters, Industrial Electronics, IEEE Transactions on 60 (4) (2013) 1271–1280.
9. M. Moafi, M. Marzband, M. Savaghebi, J. M. Guerrero, Energy management system based on fuzzy fractional order pid controller for transient stability improvement in microgrids with energy storage, International Transactions on Electrical Energy Systems (2016).
10. P. R. Almeida, F. Soares, J. P. Lopes, Electric vehicles contribution for frequency control with inertial emulation, Electric Power Systems Research 127 (2015) 141 – 150.
11. A. Raghami, M. T. Ameli, M. Hamzeh, Online droop tuning of a multi-dg microgrid using cuckoo search algorithm, Electric Power Components and Systems 43 (14) (2015) 1583–1595.
12. H. Bevrani, S. Shokoohi, An intelligent droop control for simultaneous voltage and frequency regulation in islanded microgrids, Smart Grid, IEEE Transactions on 4 (3) (2013) 1505–1513.
13. X. Lu, J. Guerrero, K. Sun, J. Vasquez, R. Teodorescu, L. Huang, Hierarchical control of parallel ac-dc converter interfaces for hybrid microgrids, Smart Grid, IEEE Transactions on 5 (2) (2014) 683–692.
14. I. Serban, C. Marinescu, Control strategy of three-phase battery energy storage systems for frequency support in microgrids and with uninterrupted supply of local loads, Power Electronics, IEEE Transactions on 29 (9) (2014) 5010–5020.
15. D. Pudjianto, M. Aunedi, P. Djapic, G. Strbac, Whole-systems assessment of the value of energy storage in low-carbon electricity systems, Smart Grid, IEEE Transactions on 5 (2) (2014) 1098–1109.
16. M. Qadrdan, H. Ameli, G. Strbac, N. Jenkins, Efficacy of options to address balancing challenges: Integrated gas and electricity perspectives, Applied Energy 190 (2017) 181 – 190.
17. E. Abbasi, H. Ameli, K. Strunz, N. Duc, Optimized operation, planning, and frequency control of hybrid generation-storage systems in isolated networks, in: Innovative Smart Grid Technologies (ISGT Europe), 2012 3rd IEEE PES International Conference and Exhibition on, 2012, pp. 1–8.
18. J. Peas Lopes, C. Moreira, A. Madureira, Defining control strategies for microgrids islanded operation, Power Systems, IEEE Transactions on 21 (2) (2006) 916–924.
19. C. Ahn, H. Peng, Decentralized voltage control to minimize distribution power loss of microgrids, Smart Grid, IEEE Transactions on 4 (3) (2013) 1297–1304.
20. A. Cagnano, E. De Tuglie, M. Liserre, R. Mastromauro, Online optimal reactive power control strategy of pv inverters, Industrial Electronics, IEEE Transactions on 58 (10) (2011) 4549–4558.
21. H. Ameli, M. T. Ameli, S. H. Hosseinian, Multi-stage frequency control of a microgrid in the presence of renewable energy units, Electric Power Components and Systems 45 (2) (2017) 159–170.
22. E. Abbasi, K. Strunz, R. Fletcher, F. Gao, N. Hatziargyriou, R. Iravani, G. Joos, Benchmark systems for network integration of renewable and distributed energy resources, in: CIGRÉ Task Force C6.04.02, 2014.
23. A. M. Hemeida, A fuzzy logic controlled superconducting magnetic energy storage, smes frequency stabilizer, Electric Power Systems Research 80 (6) (2010) 651 – 656.
24. A. Engelbrecht, Fundamentals of computational swarm intelligence, in: Hoboken, NJ: Wiley, 2005.
25. F. Shahnia, A. Ghosh, G. Ledwich, F. Zare, Voltage unbalance improvement in low voltage residential feeders with rooftop pvs using custom power devices, International Journal of Electrical Power & Energy Systems 55 (0) (2014) 362–377.
26. B. Singh, S. R. Arya, P. Verma, An implementation of double-frequency oscillation cancellation technique in control of dstatcom, International Transactions on Electrical Energy Systems 24 (6) (2014) 796–807.
27. M. Badoni, A. Singh, B. Singh, An implementation of variable step-size least-mean-square based control algorithm for dstatcom, International Transactions on Electrical Energy Systems 26 (7) (2016) 1540–1554.
28. J. Espi Huerta, J. Castello-Moreno, J. Fischer, R. Garcia-Gil, A synchronous reference frame robust predictive current control for three-phase grid-connected inverters, Industrial Electronics, IEEE Transactions on 57 (3) (2010) 954–962.
29. M. Haque, M. Negnevitsky, K. Muttaqi, A novel control strategy for a variable-speed wind turbine with a permanent-magnet synchronous generator, Industry Applications, IEEE Transactions on 46 (1) (2010) 331–339.
30. X. Sui, Y. Tang, H. He, J. Wen, Energy-storage-based low-frequency oscillation damping control using particle swarm optimization and heuristic dynamic programming, Power Systems, IEEE Transactions on 29 (5) (2014) 2539–2548.
31. Z.-L. Gaing, A particle swarm optimization approach for optimum design of pid controller in avr system, Energy Conversion, IEEE Transactions on 19 (2) (2004) 384–391.
32. S. Liu, X. Wang, P. Liu, Impact of communication delays on secondary frequency control in an islanded microgrid, Industrial Electronics, IEEE Transactions on 62 (4) (2015) 2021–2031.
33. L. A. Zadeh, Fuzzy logic = computing with words, Fuzzy Systems, IEEE Transactions on 4 (2) (1996) 103–111.
34. M. Datta, T. Senjyu, Fuzzy control of distributed pv inverters/energy storage systems/electric vehicles for frequency regulation in a large power system, Smart Grid, IEEE Transactions on 4 (1) (2013) 479–488.
35. H. Yousef, K. AL-Kharusi, M. Albadi, N. Hosseinzadeh, Load frequency control of a multi-area power system: An adaptive fuzzy logic approach, Power Systems, IEEE Transactions on 29 (4) (2014) 1822–1830.
36. I. Ngamroo, Y. Mitani, K. Tsuji, Application of smes coordinated with solid-state phase shifter to load frequency control, Applied Superconductivity, IEEE Transactions on 9 (2) (1999) 322–325.
37. P. Kundur, Power system stability and control, in: McGraw-Hill, 2006.
38. D.-J. Lee, L. Wang, Small-signal stability analysis of an autonomous hybrid renewable energy power generation/energy storage system part i: Time-domain simulations, Energy Conversion, IEEE Transactions on

23 (1) (2008) 311–320.
39. V. Nasirian, S. Moayedi, A. Davoudi, F. Lewis, Distributed cooperative control of dc microgrids, Power Electronics, IEEE Transactions on 30 (4) (2015) 2288–2303.

